communications biology

A Nature Portfolio journal

Article

https://doi.org/10.1038/s42003-025-07738-0

FOXO4-DRI induces keloid senescent fibroblast apoptosis by promoting nuclear exclusion of upregulated p53-serine 15 phosphorylation

Yu-Xiang Kong[1,2,5], Zhi-Shuai Li[1,2,5], Yuan-Bo Liu[3], Bo Pan[4], Xin Fu[1,2], Ran Xiao[1,2] ✉ & Li Yan[1,2] ✉

Keloids are pathological scars exhibiting tumour-like aggressiveness and high recurrence rate. Here we find increased proportion of pro-inflammatory and mesenchymal fibroblast subpopulations and senescent fibroblasts, and enhanced expression of senescence-associated secretory phenotype genes using single-cell RNA sequencing analysis, as well as elevated p16 protein and more β-galactosidase-positive cells in keloids. The up-regulated p53-serine15 phosphorylation (p53-pS15) in keloids is identified by phosphospecific protein microarray and western blotting. We further demonstrate that a senolytic FOXO4-D-retro-inverso-isoform peptide (FOXO4-DRI) promotes apoptosis and decreases G0/G1 phase cells in pro-senescence models of keloid organ cultures and fibroblasts, accompanied with p53-pS15 nuclear exclusion. Our study indicates that upregulation of p53-pS15 and p16 maintains a persistent senescent microenvironment to promote cell cycle arrest and apoptosis resistance in keloid fibroblasts. FOXO4-DRI shows potential as a treatment targeting the senescence and apoptosis resistance, and holds promise as an approach to prevent the aggressiveness and relapse of keloids.

Keloids form a dysregulated wound-healing process characterized by aggressive tumor-like growth beyond the boundaries of the initial insult and a high rate of recurrence. Treatments for keloids remain unsatisfactory because the key pathophysiological mechanism is unknown[1]. Currently, keloids are considered a chronic inflammatory disease with cancer-like tendencies. Multiple cytokines and inflammatory factors participate in keloid formation, such as transforming growth factor β1(TGF-β1), vascular endothelial growth factor (VEGF), interleukin (IL)-1, IL-6, and IL-8, as well as increased matrix metalloproteinases (MMP_S), which may promote fibroblast proliferation and migration, the inflammatory response, and collagen production[2–4]. Fibroblast apoptosis resistance, tumor-like stem cells, and gene dysfunction are involved in the molecular pathogenesis of local aggression and recurrence of keloids. Moreover, dysregulation of the tumor suppressor, p53, combined with upregulation of anti-apoptotic genes was linked to lower apoptosis in keloids[5,6]. Therefore, p53 is an important therapeutic target for keloids because of its crucial role in regulating apoptosis[7,8].

The p53/p21 and p16/Rb (retinoblastoma) axes are the two central signaling pathways involved in senescence regulation. p53 controls both apoptosis and senescence by promoting p21 transcription, resulting in cell cycle arrest during DNA repair. The cell apoptotic cascade is activated when the DNA damage is irreversible. p16 is crucial for maintaining senescence by regulating Rb protein phosphorylation to inhibit cell division[9]. Cellular senescence is characterized by a stable arrest in the cell cycle and encompasses a range of cellular changes that culminate in the development of a complex, pro-inflammatory secretory profile known as the senescence-associated secretory phenotype (SASP), which plays a critical role in fibrosis and tumors by affecting numerous processes, including invasion and therapy resistance[10]. Senolytic therapies may be an effective approach for preventing cancer recurrence and therapy resistance. In senescent cells, p53

[1]Research Center of Plastic Surgery Hospital, Chinese Academy of Medical Sciences and Peking Union Medical College, Ba-Da-Chu Road 33#, Beijing, 100144, PR China. [2]Key Laboratory of Tissue and Organ Regeneration, Chinese Academy of Medical Sciences, Ba-Da-Chu Road 33#, Beijing, 100144, PR China. [3]Department of Plastic and Reconstructive Surgery, Plastic Surgery Hospital, Chinese Academy of Medical Sciences and Peking Union Medical College, Ba-Da-Chu Road 33#, Beijing, 100144, PR China. [4]Auricular Plastic and Reconstructive Surgery Center, Plastic Surgery Hospital, Chinese Academy of Medical Sciences and Peking Union Medical College, Ba-Da-Chu Road 33#, Beijing, 100144, PR China. [5]These authors contributed equally: Yu-Xiang Kong, Zhi-Shuai Li.
✉e-mail: xiaoran@psh.pumc.edu.cn; yanli@psh.pumc.edu.cn

localizes to DNA segment with chromatin alterations reinforcing senescence (DNA-SCARS). This p53 is phosphorylated on Serine 15 (p53-pS15), which prevents its degradation by MDM2[11]. The transcription regulator, forkhead box class O isoforms 4 (FOXO4), maintains the viability of senescent cells by localizing adjacent to p53-pS15 to prevent the nuclear exclusion of active p53-pS15 to mediate apoptosis[11]. In FOXO4-DRI (D-retro-inverso-isoform peptide), L-amino acids are substituted by D-amino acids that mimic the FOXO4 p53 binding domain. Senolytic FOXO4-DRI can inhibit FOXO4 binding by disrupting the p53-FOXO4 interaction and selectively cause apoptosis via p53 nuclear exclusion in senescent cells and aging mouse models, which may be a promising approach for preventing senescence[11].

Senescent cells express senescence-associated (SA) biomarkers, such as SA-β-galactosidase, p53, p21, and p16. The SASP is highly cell specific and diverse secreted factors; however, VEGF, IL-1a, IL-6, IL-8, MMPs, and chemokines (CXCL2, CXCL3) are secreted by most senescent cells[10,12]. In previous studies, cellular senescence has been considered a mechanism of preventing abnormal proliferation to malignancy in keloids and could be used to halt the progression of keloids[13]. Recently, the obvious senescence phenotypes in keloid lesions and fibroblasts were found and senolytic dasatinib was demonstrated to have antifibrotic effects in keloids[14,15]. However, the underlying mechanism of cellular senescence in keloids remain unclear. Additionally, it is unknown whether senolytic FOXO4-DRI can be used to treat keloids.

In the present study, we investigated the expression of SA markers and their regulatory proteins in keloids. Differences in the phosphoprotein profiles of the signaling pathway in keloid fibroblasts were detected, and the expression of p53-pS15 and FOXO4 was examined in fibroblasts and keloid tissues. Furthermore, the apoptosis-inducing effect and mechanism of FOXO4-DRI in a serum limitation-induced senescent fibroblast and organ culture models of keloids were examined.

Our results provide a possible mechanism in which upregulation of phosphorylated p53 and p16 maintain the cell cycle arrest of keloid fibroblasts, and FOXO4-DRI selectively induces apoptosis of keloid senescent fibroblasts by prompting p53-pS15 nuclear exclusion.

Results

Senescence-associated markers were enhanced in keloid fibroblasts and lesions

Analysis of the heterogeneity of keloid cells revealed 28 cellular clusters (0–27) using unsupervised clustering of 34,043 cells based on established lineage-specific marker genes (Supplementary Fig. 1a). Clusters 0 and 9 displayed more obvious fibroblast cluster-specific genes, *PDGFRA* and *DCN*, that were defined as the fibroblast lineage markers according as previously described (Supplementary Fig. 1b)[16]. Secondary clustering of fibroblasts further identified four subpopulations[17] (Supplementary Fig. 1c), the proportions of mesenchymal and pro-inflammatory subpopulations were increased in keloids (51% and 31%, respectively) versus those in normal skin (34% and 25%, respectively) (Fig. 1a). Compared with those in normal skin fibroblast subpopulations, the expression levels of senescence- and inflammation-associated genes, including *p16* (also known as *CDKN2A*), *SFRP4*[18], *IGF1*[19], and *IL1R1* were increased in keloid mesenchymal fibroblasts, whereas *CCND2*, *IL-6*, *CXCL3*, and *IL1R1* were increased in keloid pro-inflammatory fibroblasts (Fig. 1b). These results indicated that mesenchymal progenitor like and pro-inflammatory fibroblasts were involved in keloids senescence which may play crucial roles in the aggression and recurrence of keloids.

To investigate the difference in proportion of senescent fibroblasts between in keloids and normal skins. The unsupervised clustering of 4453 fibroblasts was used to analyze the senescent cells in keloid and normal skin fibroblast based on senescence-associated marker genes, *CDKN2A, TP53, CDKN1A* (also known as *p21*), *LMNB1, H2AFX, TP53BP1, SFRP4, CCND1* and *GLB1* according as previously reference[20,21]. The results showed that the proportion of senescence-associated markers positive cells was enhanced in keloid fibroblasts (59.5%) versus normal skin fibroblasts (36.5%) (Fig. 1c).

To detect cellular senescence in keloids, we examined SA markers. More SA-β-gal-positive stained (SA-β-gal$^+$) cells were observed in keloid lesions compared with those in adjacent or completely normal skin (Fig. 2a). Immunohistochemical staining showed higher expression of p16 in keloids than that in normal skin ($p = 0.01$; Fig. 2b). The protein level of significantly increased p16 was confirmed in keloid lesions and fibroblasts based on western blot analysis ($p = 0.0007$, $p = 0.03$; Fig. 2c, d). However, the expressions of p53 and p21 did not significantly differ in keloid lesions and fibroblasts compared to that in normal skin ($p > 0.05$, Fig. 2b–d). The data indicated that more cells showed senescent phenotype in keloids.

p53-pS15 is involved in regulating cell cycle arrest and apoptosis resistance in keloids

Phospho-specific protein microarray was used to investigate the cell signaling profile in fibroblasts from keloid versus those from adjacent skin. The results showed that among phosphoproteins, 24 were upregulated (FC ≥ 1.2) and 52 were downregulated (FC ≤ 0.83) in fibroblasts from keloid versus those from adjacent skin (Supplementary Data 1). Approximately 15%, 18%, and 20% differentially expressed phosphoproteins are involved in the p53, cell cycle, and apoptosis pathways, respectively (Fig. 3a), among which, p53-pS15 was upregulated in keloid fibroblasts (FC = 1.3). In the p53 and apoptosis pathways, G2 arrest stabilization related BCL-XL (phospho-Ser62) protein was increased (FC = 1.24)[22], pro-apoptotic B-cell lymphoma 2 (BCL2)-associated X protein (BAX; phospho-Thr167)[23] and the maintenance of S phase checkpoint related BID (phospho-Ser78)[24] protein were decreased (FC = 0.83 and 0.72) (Fig. 3b). These results suggested that the regulatory signaling of cell cycle arrest and apoptotic resistance were enhanced in keloid fibroblasts. Western blot analysis showed that the protein expression of p53-pS15 in the nuclei of keloid fibroblasts was significantly higher than that in normal skin fibroblasts ($p = 0.01$; Fig. 3c). The expression of FOXO4 in the cytoplasm of keloid fibroblasts was significantly lower than that in normal skin fibroblasts ($p = 0.03$; Fig. 3c).

Additionally, positive p53-pS15 staining fibroblasts was greater in the dermis of keloids than that in normal skin (Fig. 4a). Semi-quantitative analysis of the immunohistochemical staining and western blotting results showed a significant increase in the expression of p53-pS15 in keloids ($p = 0.0007$, $p = 0.002$; Fig. 4a, b). The data indicated that more cells in keloids underwent pro-senescence regulation.

FOXO4-DRI eliminated fibroblasts in G0/G1 phase cell cycle arrest and selectively induced senescent keloid cells apoptosis in an in vitro model of fibroblasts and organ culture

In the serum limitation-induced senescent fibroblast model, more SA-β-gal-positive cells were observed in keloid fibroblasts compared with that in normal skin fibroblasts (Fig. 5a), and the percentage of keloid fibroblasts in G0/G1 phase (90.78% ± 1.62%) was significantly higher compared with that in normal skin fibroblasts (75.47% ± 4.62%) ($p = 0.03$; Fig. 5b–d). At 3 days after adding FOXO4-DRI (25 μM) in medium, few SA-β-gal-positive cells were observed in both keloid fibroblasts and normal skin fibroblasts (Fig. 5a), and G0/G1-phase fibroblasts of keloids and normal skins decreased from 90.78% ± 1.62% to 63.68% ± 11.16%, and from 75.47% ± 4.62% to 49.4% ± 8.95%, respectively ($p = 0.002$ and $p = 0.003$, respectively; Fig. 5b–d). The percentage of apoptotic fibroblasts in keloids and normal skins increased from 3.31% ± 0.46% to 18.6% ± 9.44% and from 5.51% ± 3.34% to 25.42% ± 5.82%, respectively ($p = 0.04$ and $p = 0.01$, respectively; Fig. 6a–c).

However, in the non-senescent control fibroblast model cultured in 10% FBS DMEM treated with or without FOXO4-DRI (25 μM), no SA-β-gal-positive cells were observed both in keloid fibroblasts and in normal skin fibroblasts (Supplementary Fig. 2a), and the percentage of fibroblasts in G0/G1 phase and the percentage of apoptotic fibroblasts did not significantly differ both in keloid fibroblasts and in normal skin fibroblasts ($p = 0.4$, Supplementary Fig. 2b–d; $p = 0.55$, Supplementary Fig. 3a–c).

To assess the half maximal inhibitory concentration (IC50) of FOXO4-DRI on the serum limitation-induced senescent fibroblast and the non-senescent control fibroblast, the fibroblast viability in the 2% FBS induced

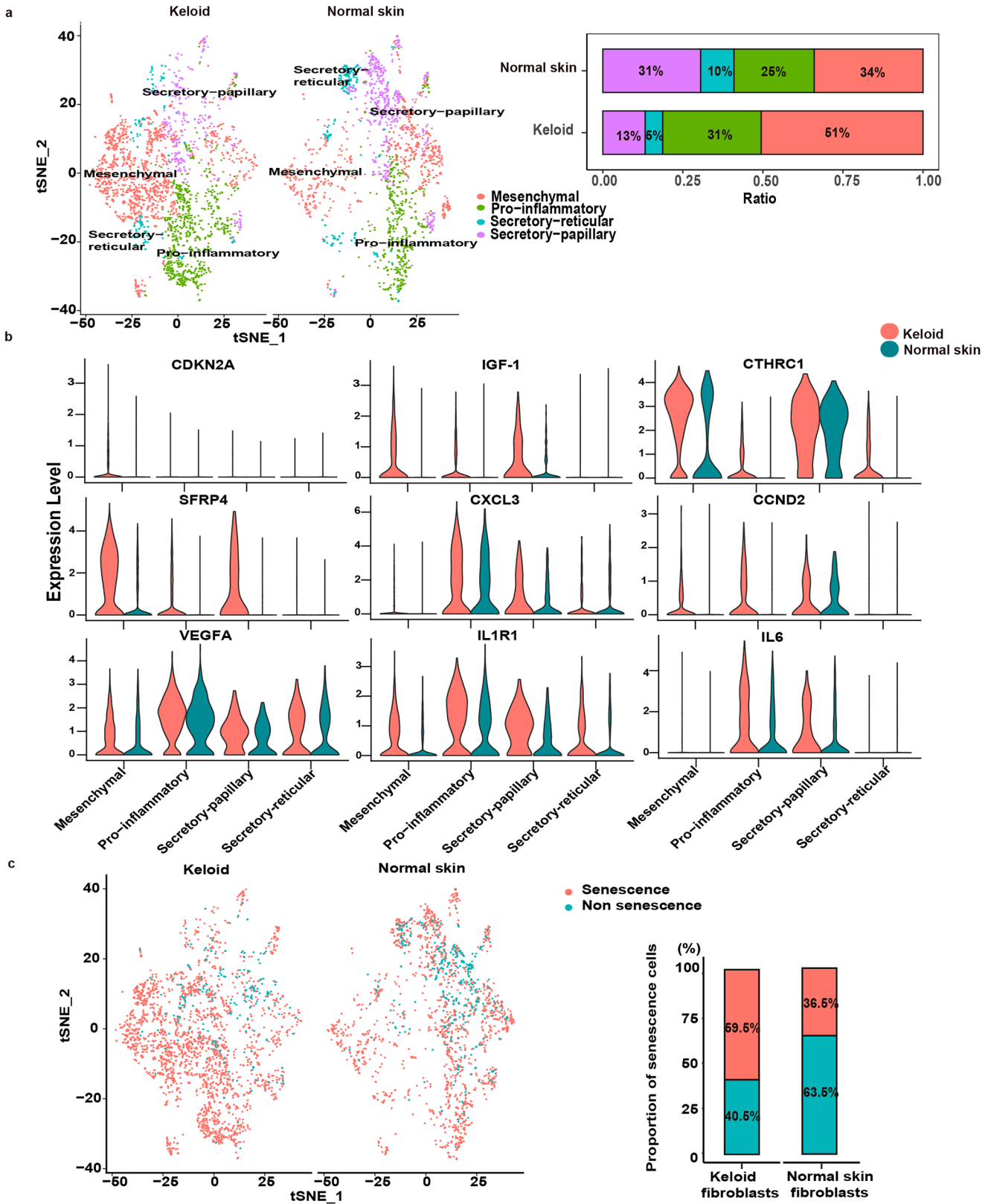

Fig. 1 | Single-cell RNA sequencing (scRNA-seq) analysis of fibroblasts derived from keloids and adjacent normal skins. a Cellular heterogeneity of fibroblasts in keloid and adjacent normal skin samples ($n = 4$). The keloid and normal skin fibroblasts were subclustered into four subpopulations: secretory-papillary, secretory-reticular, mesenchymal, and pro-inflammatory. Each fibroblast subcluster is defined on the right in different colors. The proportions of four fibroblast subpopulations in keloid and normal skin samples. **b** Violin plots showing representative differentially expressed senescence- and inflammation-related genes between keloid fibroblasts and normal skin fibroblasts subpopulations ($n = 4$). **c** t-SNE plots and bar plots showing the proportion of senescent fibroblasts in keloids and normal skins. Keloid: keloid fibroblasts, Normal skin: normal skin fibroblasts ($n = 4$).

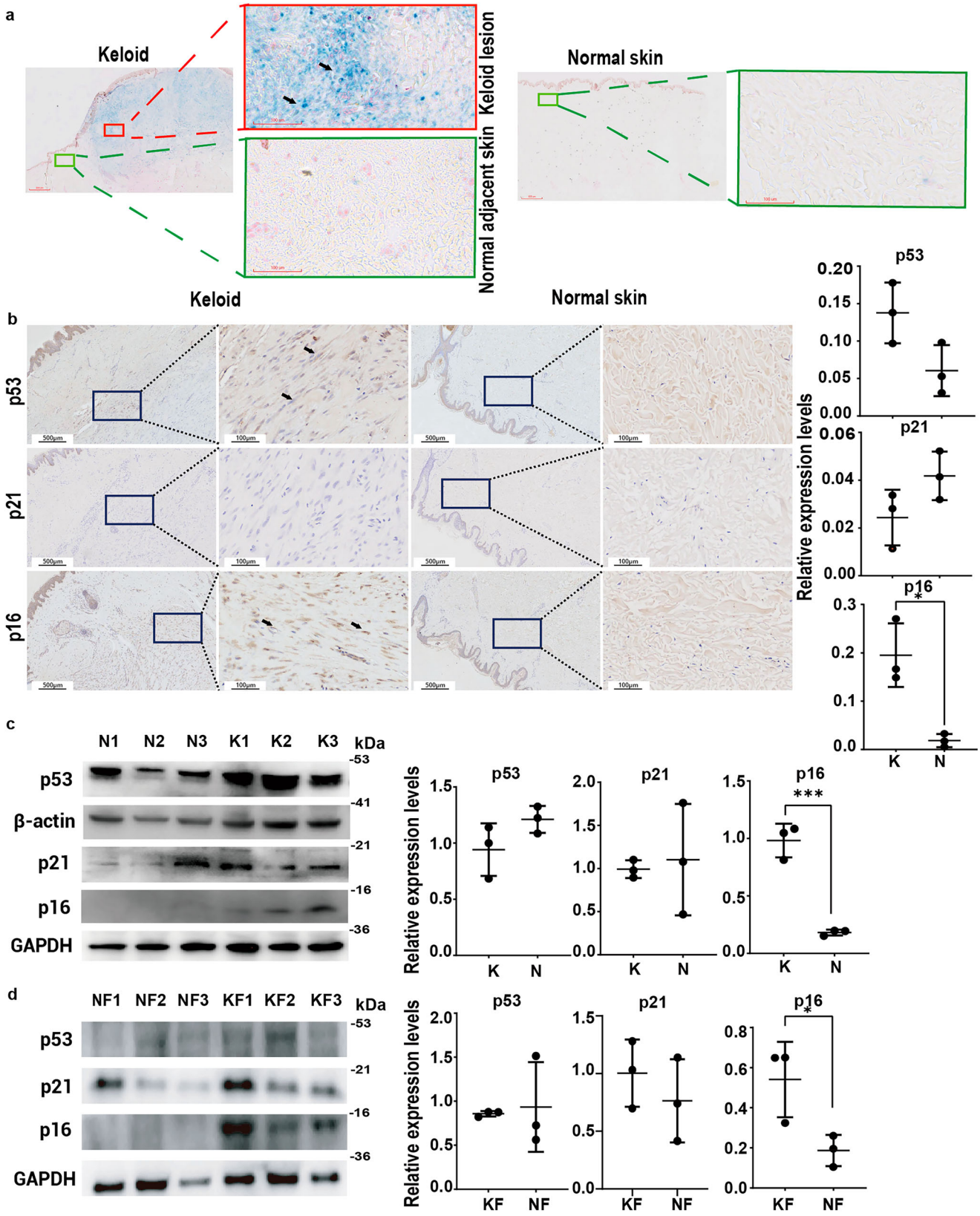

senescent fibroblast and 10% FBS cultured non-senescent control fibroblast with increasing concentrations of FOXO4-DRI was detected, and the cell viability curves were showed in Supplementary Fig. 3d. IC50 was 34.19 μM, 61.53 μM in the senescent fibroblasts from keloid and normal skin, and 93.77 μM, 104.6 μM in non-senescent control fibroblasts from keloid and normal skin, respectively. The results indicate that FOXO4-DRI potently and selectively reduces the viability of senescent fibroblasts compared to non-senescent controls (2.7-fold and 1.7-fold difference for keloid and normal skin, respectively).

Furthermore, keloid tissues were cultured in the medium containing 2% FBS, and in situ TUNEL staining was performed (Fig. 6d). The apoptotic cells were observed after 3 days culture in both groups. Compared to the

Fig. 2 | Expression of senescence-associated markers in fibroblasts and tissues from keloids and normal skins. a Histological sections of normal skins and keloids were detected using senescence-associated β-galactosidase (SA-β-gal) staining, and nuclei were counterstained with nuclear fast red. Specific keloid disease lesion sites consist of normal adjacent skin (green) and keloid lesion (red) sites. Image of SA-β-gal expression in keloid lesion, normal adjacent skin, and normal skin based on panoramic scan (red bar = 800 μm). Red-boxed inserts show positive expression of SA-β-gal (black arrowheads) in the keloid lesion dermis and green-boxed inserts show expression of SA-β-gal in the normal adjacent skin and normal skin dermis (red bar = 100 μm). **b** Histological sections of normal skins and keloids were detected using immunohistochemical staining and semi-quantitative analysis for senescence-associated markers p53, p16, and p21 in brown, and nuclei were counterstained with haematoxylin-eosin (H/E) in blue (scale bar = 500 μm). Black-boxed inserts show the expression of p53, p16, and p21 in fibroblasts of keloids and normal skins dermis (black arrowheads, scale bar = 100 μm). The protein expression levels of p53, p16, and p21 in tissues (**c**) and fibroblasts (**d**) from keloids and normal skins detected using western blot analysis. (K keloid tissue, N normal skin tissue, KF keloid fibroblasts, NF normal skin fibroblasts) Data shown as the means ± SD ($n = 3$; $^{*}p < 0.05$, $^{***}p < 0.001$).

negative control group, positive TUNEL staining cells began decreasing at 7 days and few apoptotic cells were observed at 10 days in FOXO4-DRI (25 μM) addition group.

These data suggested that fibroblasts from keloids and normal skins were arrested in G0/G1 phase by serum-limitation culture and showed the senescent phenotype, moreover, keloid fibroblasts were susceptible to senescent stimulus. And FOXO4-DRI selectively induced apoptosis of senescent keloid cells at the same clearance efficiency as in normal skin fibroblasts.

FOXO4-DRI prompted relocation of p53-pS15 and FOXO4 in the serum limitation-induced senescent fibroblast model

Double immunofluorescence staining was performed to investigate the distribution of p53-pS15 and FOXO4 in serum limitation-induced senescent fibroblasts model with or without treatment with FOXO4-DRI (Fig. 7). Clear and strong localization of p53-pS15 and FOXO4 was observed in the nuclei of keloid fibroblasts. After serum limitation-induction, positive FOXO4 and p53-pS15 immunofluorescence staining was stronger in the nucleus of keloid fibroblasts at 48 h, but in the nucleus of normal skin fibroblasts at 72 h. After FOXO4-DRI treatment, the staining of FOXO4 and p53-pS15 became weaker in the nucleus at 48 h and then disappeared with an accumulation in the cytoplasm at 72 h, especially in keloid fibroblasts. These results suggested that keloid fibroblasts underwent pro-senescence regulation earlier compared with normal skin fibroblasts via p53-pS15 under serum limitation stimulus, and p53-pS15 and FOXO4 translocated from the nucleus to the cytoplasm during FOXO4-DRI treatment.

To detect the expression of p53, p53-pS15, FOXO4 after FOXO4-DRI treatment in the serum limitation-induced senescent fibroblast model, the western blot analysis was used, and the results indicate no significant difference in the expressions of these proteins in fibroblasts from keloids and normal skins treated with FOXO4-DRI (25 μM) compared to those untreated, suggesting that the apoptotic effect of FOXO4-DRI in senescent keloid cells might be location-dependent rather than solely based on expression levels of these proteins ($p > 0.05$, Supplementary Fig. 4).

Discussion

Cellular senescence has been implicated in various biological processes including cancer and tissue repair. Senescent stimuli endow cells with resistance to apoptosis, which involves high activity of anti-apoptotic molecules, such as BCL2 and BCL-XL, and reduced pro-apoptotic BAX protein. Moreover, phospho-BCL-XL (Ser62) stabilizes G2 arrest by binding to and co-localizing with Cdk1 (cdc2) in nucleolar structures to avoid rapid nucleolar disassembly associated with mitosis onset, playing an unexpected role in the G2 phase checkpoint downstream of DNA damage distinct from its anti-apoptotic function[22]. Therapy-induced senescent cells can re-enter the cell cycle to show aggressive proliferative and cancer stem-like properties, presenting a risk for recurrence and treatment resistance. Failure to clear senescent cells also lead to a pro-tumorigenic microenvironment characterized by chronic inflammation because of the SASP[12,25]. Hence, senolytic therapies may be a suitable approach for increasing therapy sensitivity and preventing cancer relapse[10]. In our study, we demonstrated a persistent senescent-inflammatory microenvironment and a p53-serine 15 phosphorylation regulatory mechanism in keloids, which may play crucial roles in the aggression and recurrence of keloids. Moreover, FOXO4-DRI was used to selectively induce apoptosis of senescent fibroblasts in both keloid fibroblast and organ culture senescent models, showing potential as a treatment that targets the senescence and apoptosis resistance observed in keloid fibroblasts.

The discrepancy in the reports of p53 expression in keloids[5,26,27] suggests that the regulatory functions of p53 in keloid fibroblasts depends on activities rather than expression levels of p53. p53-pS15 is a major focal point in p53 activation to mediate p53-dependent transcription or growth arrest, Ser 15 phosphorylation triggers a sequence of additional sites phosphorylation in p53 (including Ser9, -20, -46 and Thr18) that contribute further to p53 activation[28]. Our study suggests that the increased expression and nuclear distribution of p53-pS15 in keloids are associated with the promotion of pro-senescence regulation causing the cell cycle arrest and resistance to apoptosis. Compared with normal skin fibroblasts, a greater number of keloid fibroblasts displayed a senescent phenotype and were arrested at the G0/G1 phase using a serum-limited culture approach, indicating the senescent tendency of keloid fibroblasts under simulated ischemic stress.

When p53 is inactivated, the accumulation of DNA damage leads to sustained senescence induction through p16 expression[29]. p16 and p53 mediate senescence as complementary pathways to control tumor development. We observed no significant changes in the expression of p53 or p21 in keloid lesions or fibroblasts compared to those in normal skin. The p53/p21 pathway may not be responsible for maintaining senescence after upregulation of p53-pS15 initiates senescence in keloids. However, p21 activates Rb to produce a bioactive secretome that places stressed cells under immunosurveillance. This action causes macrophages to polarize towards an M1 phenotype and lymphocytes mount a cytotoxic T cell response to eliminate target cells[30]. Whether the p53/p21 axis was involved in keloid immunosurveillance requires further analysis.

Low apoptotic rates and overexpression of the anti-apoptotic gene, *BCL2*, are considered as important pathogeneses of invasion and recurrence of keloids[5,31]. Therefore, pro-apoptotic therapy is a promising approach for preventing the invasion and recurrence of keloids. Senolytic therapies targeting anti-apoptotic pathways can eliminate senescent cells and enhance chemoradiotherapy efficacy of cancer[10,32]. Dasatinib has shown antifibrotic effects in keloid fibroblasts and xenotransplant keloid tissue in mice through the selective clearance of senescent cells and modulation of SASP, implying that dasatinib can be possibly used for senolytic treatment of keloids[15].

Hypoxia and inflammation activate p53 via phosphorylation. p53-pS15 combined with FOXO4 in the nucleus of senescent cells inhibits p53 into the cytoplasm to mediate apoptosis and halt the cell cycle[9,11]. FOXO4-DRI reduces chemotherapy-induced senescence and chemotoxicity and cellular senescence in p16-positive aging XpdTTD/TTD mice[11]. In our study, FOXO4-DRI selectively induced apoptosis in senescent keloid fibroblasts by promoting the relocation of p53-pS15 from the nucleus to the cytoplasm, exhibiting similar clearance efficiency to that in normal skin fibroblasts.

In summary, we observed a persistent pro-senescent microenvironment prompted cell cycle arrest and apoptotic resistance in keloids; keloid fibroblasts were prone to senescence following an ischemic stimulus, and FOXO4-DRI selectively induced the apoptosis of keloid senescent fibroblasts via p53-pS15 translocation from the nucleus to the cytoplasm. Therefore, FOXO4-DRI shows potential as a keloid treatment to prevent the

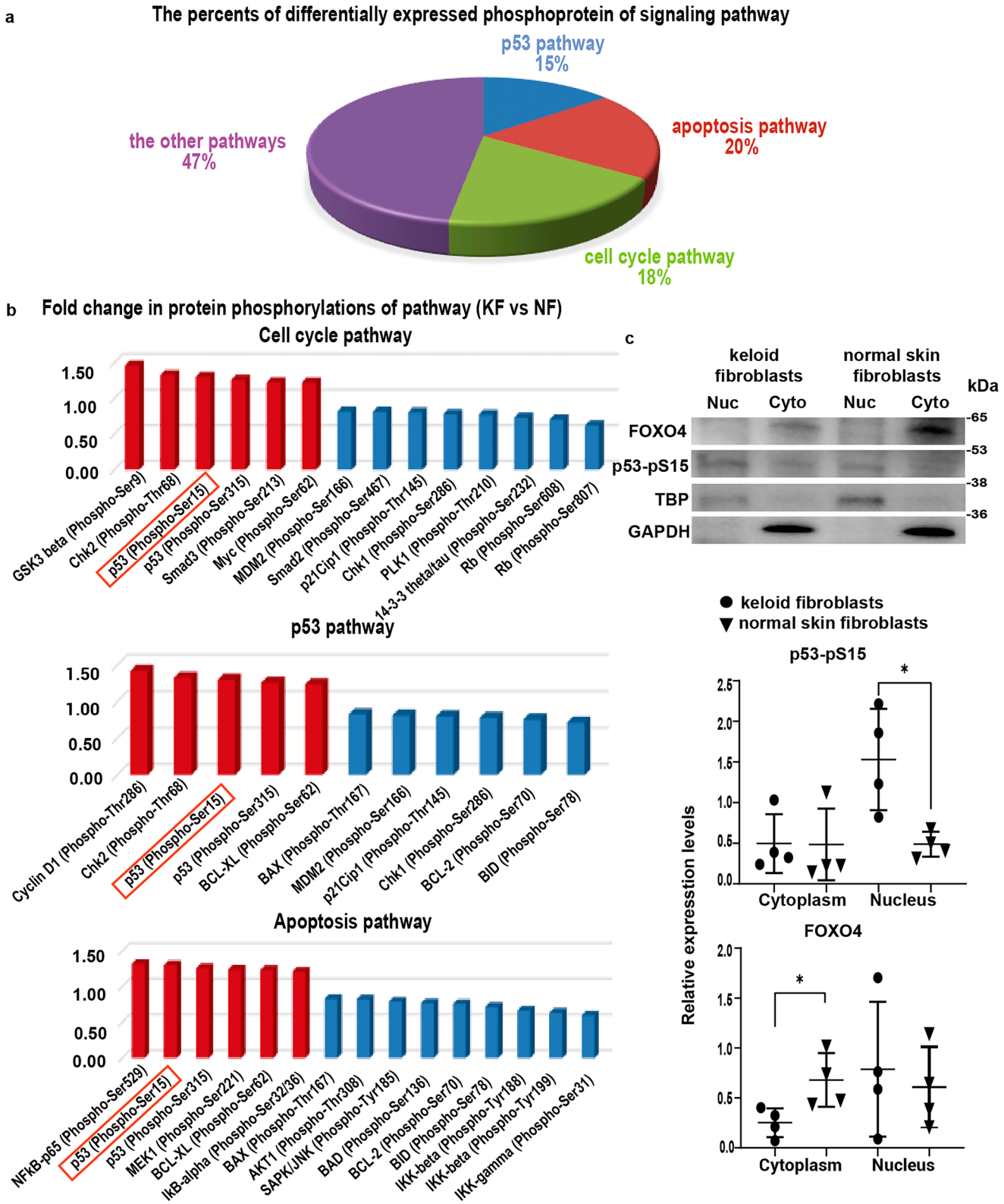

Fig. 3 | Differential expression of phosphoproteins and p53-pS15 and FOXO4 in fibroblasts from keloids and normal skins. Phosphoprotein expression profiles were detected using the CSP 100 plus phospho-specific protein microarray (Full Moon Microsystems). **a** Percentage of differentially expressed phosphoproteins in p53, apoptosis, and cell cycle signaling pathway. **b** The fold-change (FC) of differentially expressed phosphoproteins (FC ≥ 1.2 or FC ≤ 0.83) in cell cycle, p53, and apoptosis signaling pathway in keloid fibroblasts versus in normal adjacent skin fibroblasts. **c** Protein expression levels of p53-pS15 and FOXO4 in the nucleus and cytoplasm of keloid fibroblasts and normal skin fibroblasts detected using western blot analysis. (Nuc Nucleus, Cyto Cytoplasm) Data are shown as the means ± SD ($n = 4$; $^*p < 0.05$).

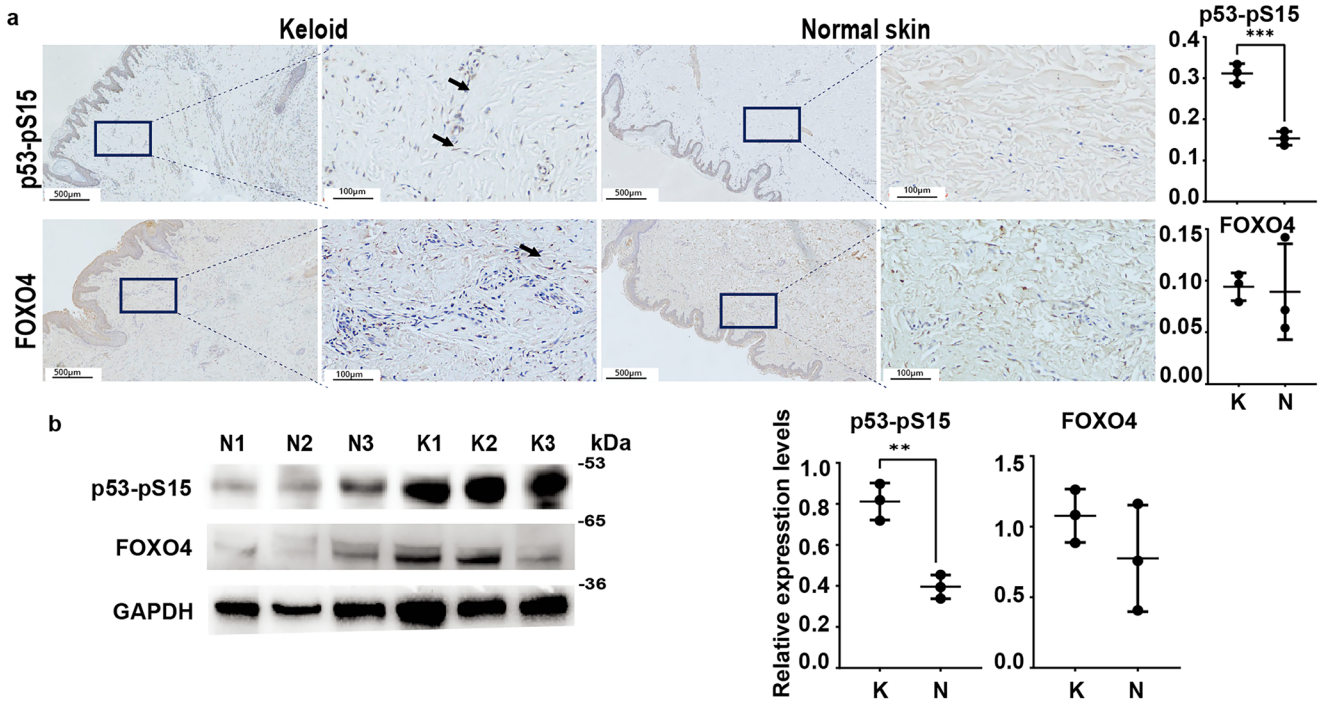

Fig. 4 | The expressions of p53-pS15 and FOXO4 in keloid and normal skin tissues. a Immunohistochemical staining and semi-quantitative analysis of normal skin and keloid sections for p53-pS15 and FOXO4 in brown and nuclear counter-staining in blue (scale bar = 500 μm). Black-boxed inserts show the expression of p53-pS15 and FOXO4 (black arrowheads) in fibroblasts of keloid dermis and normal skin dermis (scale bar = 100 μm). **b** Protein expression levels of p53-pS15 and FOXO4 in keloid and normal skin tissues detected using western blot analysis. N normal skin tissues, K keloid tissues. Data are shown as the means ± SD ($n = 3$; $^{**}p < 0.01$, $^{***}p < 0.001$).

aggressiveness and relapse of keloids by alleviating the inflammatory microenvironment.

Methods

Specimens

Keloid and normal skin samples were obtained from patients who underwent plastic surgery for keloids or reconstructive surgery for patients without keloids. The patient data are presented in Table 1. The additional content of clinical features of specimens are showed in Supplementary Table 1. All experiments were approved by the Ethics Committee of the Plastic Surgery Hospital (Chinese Academy of Medical Sciences and Peking Union Medical College, Beijing, China; approval number: 2021-179), and all donors provided informed consent. All ethical regulations relevant to human research participants were followed.

Analysis of single-cell RNA sequencing

Single-cell RNA sequencing (scRNA-seq) data (HRA000425) were downloaded from Genome Sequence Archive (SRA)-Human databases in China National Center for Bioinformation[16], converted into FASTQ format using fasterq-dump software (sratoolkit 3.0.2, NCBI, NIH, Bethesda, MD, USA), converted into a matrix data file using Cell Ranger software version 3.0.2 (10xGenomics, Pleasanton, CA, USA), converted into Seurat objects using Seurat 5.0.1 software (Satija lab, Lower Manhattan, New York, NY, USA), and plotted for *t*-distributed stochastic neighbor embedding (*t*-SNE) visualization. The cells from four keloid and four adjacent normal skin samples were unsupervised and clustered. The expression of genes in the fibroblast subclusters was analyzed using FeaturePlot and VlnPlot methods in Seurat.

Histochemical and immunohistochemical staining

Tissue cryosections were fixed for 15 min, incubated with SA-β-gal staining at 37 °C overnight in the dark according to the manufacturer's instructions (Solarbio, Beijing, China). Paraffin sections were immunohistochemically stained using standard procedures. The specific primary antibodies were shown in Table 2. Super Vision Two-Step Polymer Non-Biotin HRP Detection System for DAB (Boster, Wuhan, China) was used for secondary antibody staining according to the manufacturer's instructions. Sections were imaged using an EasyScan NFC microscope (Motic, Hong Kong, China).

Phospho-specific protein microarray detection

A CSP 100 plus phospho-specific protein microarray (Full Moon Microsystems, Sunnyvale, CA, USA) was used to investigate the cell signaling profile. This microarray contains 304 antibodies against 147 phosphorylation sites of proteins involved in 16 signaling pathways. The experiment was performed and data were analyzed by Wayen Biotechnologies (Shanghai, China). A fold-change (FC) ≥ 1.2 or FC ≤ 0.83 in the experimental group compared with that in the control group was considered as up- or down-regulation of phospho-specific proteins.

Serum limitation-induced senescent fibroblasts model and effect of FOXO4-DRI

Passage 3 fibroblasts derived from keloids and normal skins were cultured in a Dulbecco's Modified Eagle's medium (DMEM, Hyclone, Logan, Utah, USA) containing 10% fetal bovine serum (FBS, Gibco, Grand Island, NY, USA) to 90% confluence, and then cultured in a DMEM containing 2% FBS for 3 days to construct a serum limitation-induced senescent fibroblast model.

FOXO4-DRI peptide consists of the following amino acid sequence in D-Isoform: ltlrkepaseiaqsileaysqngwanrrsggkrpppprrrqrrkkrg (Acetate Salt). The modification of peptide is allD-AA, Acetate Salt. Molecular weight (MW): 5358.05. It was manufactured by NovoPro Bioscience Inc (Shanghai, China) at >95% purity and stored at −20 °C in lyophilized powder until used to avoid repeated freeze-thawing. For experiments FOXO4-DRI was dissolved in DMEM to generate a 2.5 mM stock solution. The final concentration of 25 μM FOXO4-DRI was added to the cells in a DMEM containing 2% FBS or 10% FBS. The duration of treatment was 3 days.

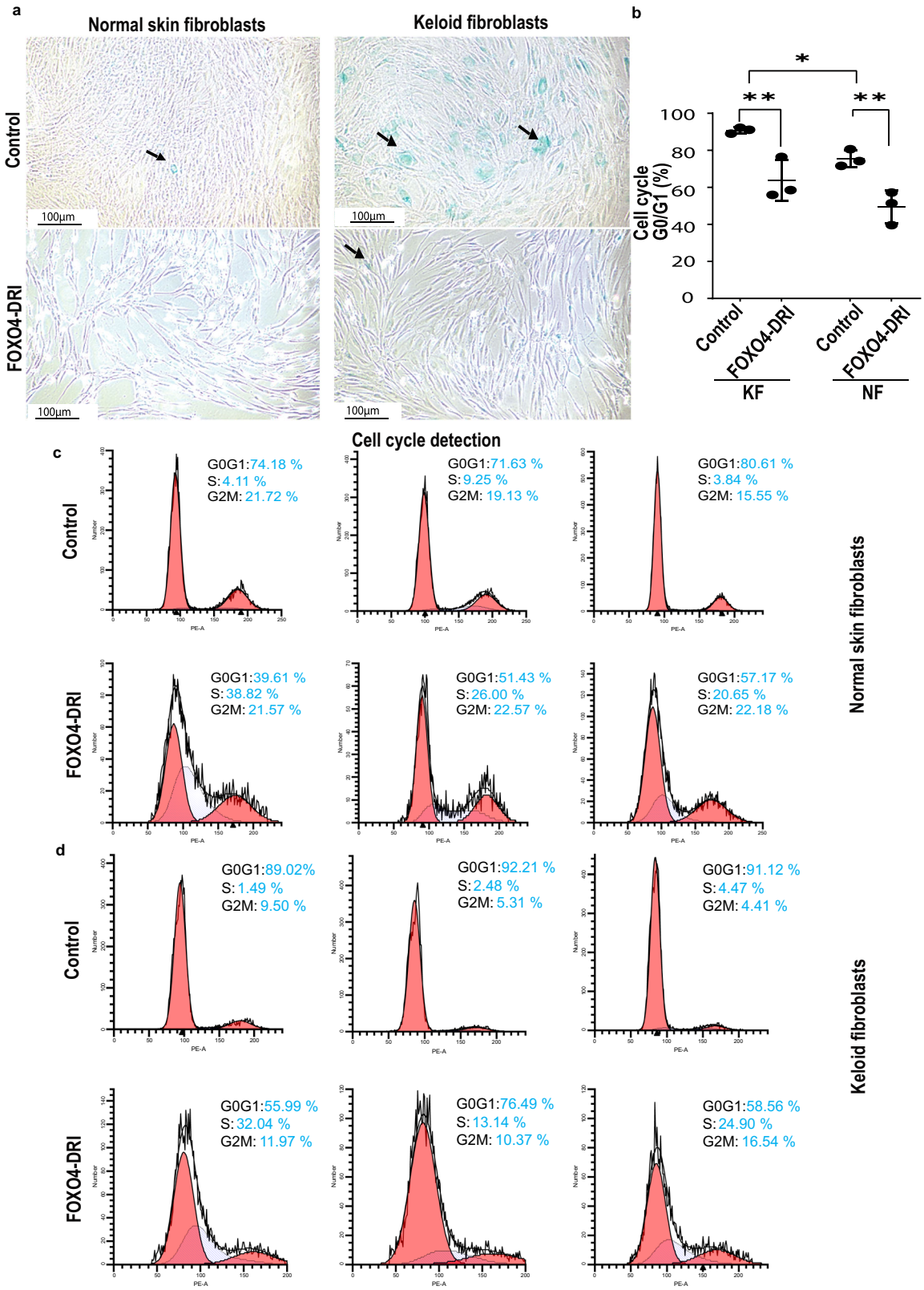

Fig. 5 | Effect of FOXO4-DRI on the senescent fibroblast model of keloids induced by serum-limitation in vitro. Fibroblasts derived from keloids and normal skins were cultured in medium containing 2% FBS for 3 days to construct the serum limitation-induced senescent fibroblast model. FOXO4-DRI (25 μM) was added to the medium and the cells were cultured for 3 days. **a** Cells were detected using SA-β-gal staining. Black arrowheads showed the blue positively stained cells for SA-β-gal (scale bar = 100 μm). Fibroblasts were detected using PI/RNase Staining Buffer for cell cycle detection. **b** Percentage of G0/G1 phase cells. (KF keloid fibroblasts, NF normal skin fibroblasts) Graphs of cell cycle detection are shown in (**c**) and (**d**). Data are shown as the means ± SD ($n = 3$; $^{*}p < 0.05$, $^{**}p < 0.01$).

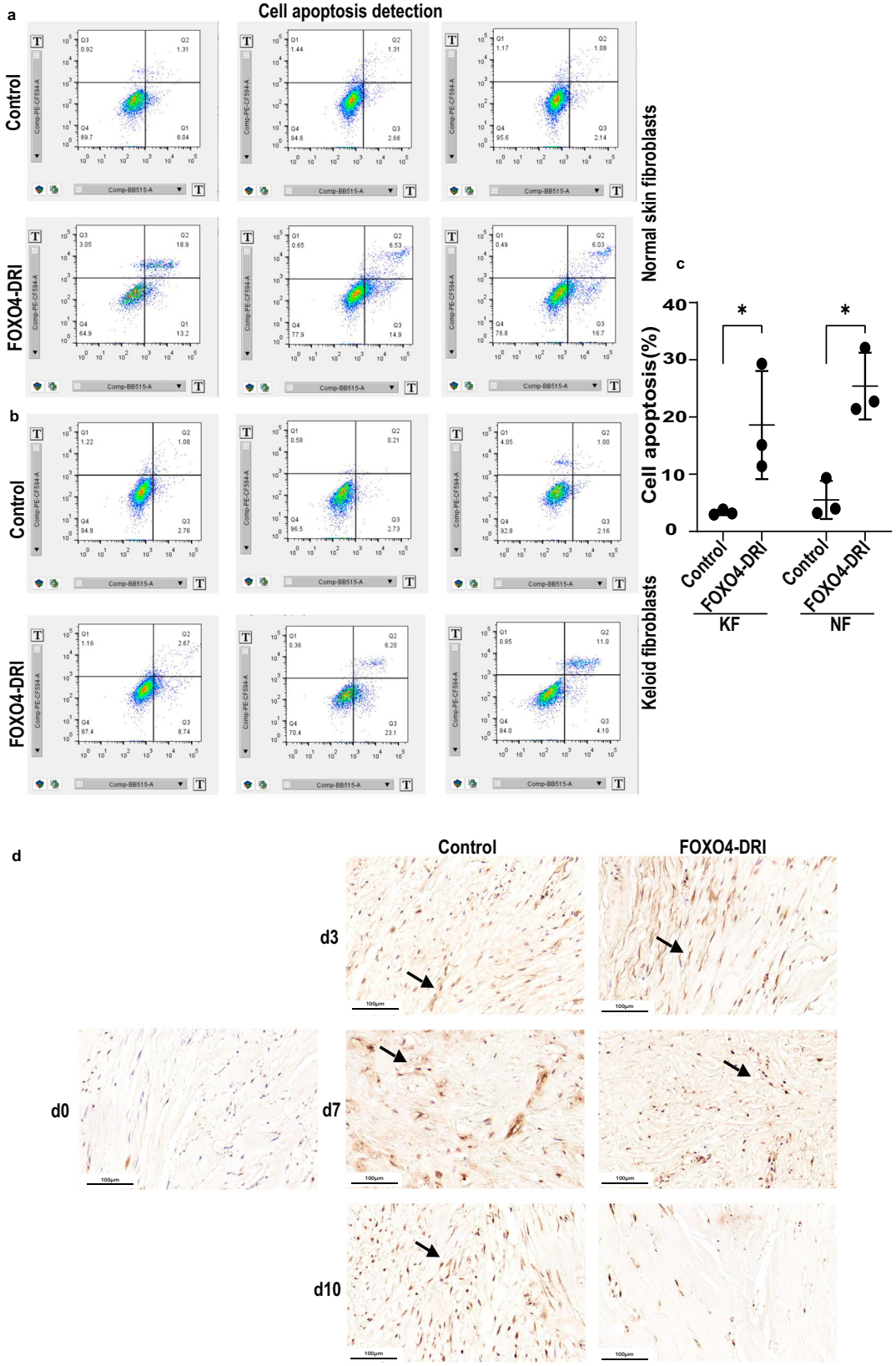

Untreated cells in 2% or 10% FBS DMEM for 3 days were used as negative controls. After treatment, cells were immediately analyzed for apoptosis and the cell cycle using a BD FACSCelesta Cell Analyzer with an Annexin V-FITC/PI Apoptosis Detection Kit and PI/RNase Staining Buffer (BD Biosciences, Franklin Lakes, NJ, USA), respectively, according to the manufacturer's instructions.

Cell viability assays

The cells were plated in triplicate in 96-well plates (4000 cells cultured in 2% FBS DMEM and 2000 cells cultured in 10% FBS DMEM). Cell viability was assessed 3 days after treatment with FOXO4-DRI at 0, 12.5, 25, 50, and 100 μM, respectively, using the Cell Counting Kit-8 (CCK-8) Assay (Dojindo, Rockville, MD, United States). Ten ul of CCK-8 solution in 100 ul

Fig. 6 | Pro-apoptotic effect of FOXO4-DRI on the senescent fibroblast and organ culture model of keloids. Fibroblasts derived from keloids and normal skins were cultured in medium containing 2% FBS for 3 days to construct the serum limitation-induced senescent fibroblast model. FOXO4-DRI (25 μM) was added to the medium and the cells were cultured for 3 days. Fibroblasts were detected using an Annexin V-FITC/PI Apoptosis Detection Kit. Graphs of cell apoptosis detection are shown in (**a**) and (**b**). **c** Percentage of apoptotic cells. (KF keloid fibroblasts, NF normal skin fibroblasts) **d** Keloid tissues were cultured with medium containing 2% FBS for 10 days to construct the serum limitation-induced senescent organ culture model. FOXO4-DRI (25 μM) was added to the medium of the organ culture model. In situ apoptotic staining of keloid organ culture with or without FOXO4-DRI (25 μM) using TUNEL; apoptotic cells in the histological sections were detected at 0, 3, 7, and 10 days. The results are shown in brown (black arrowheads). The nucleus was counterstained with haematoxylin and eosin (scale bar = 100 μm). Data are shown as the means ± SD ($n = 3$; $^*p < 0.05$).

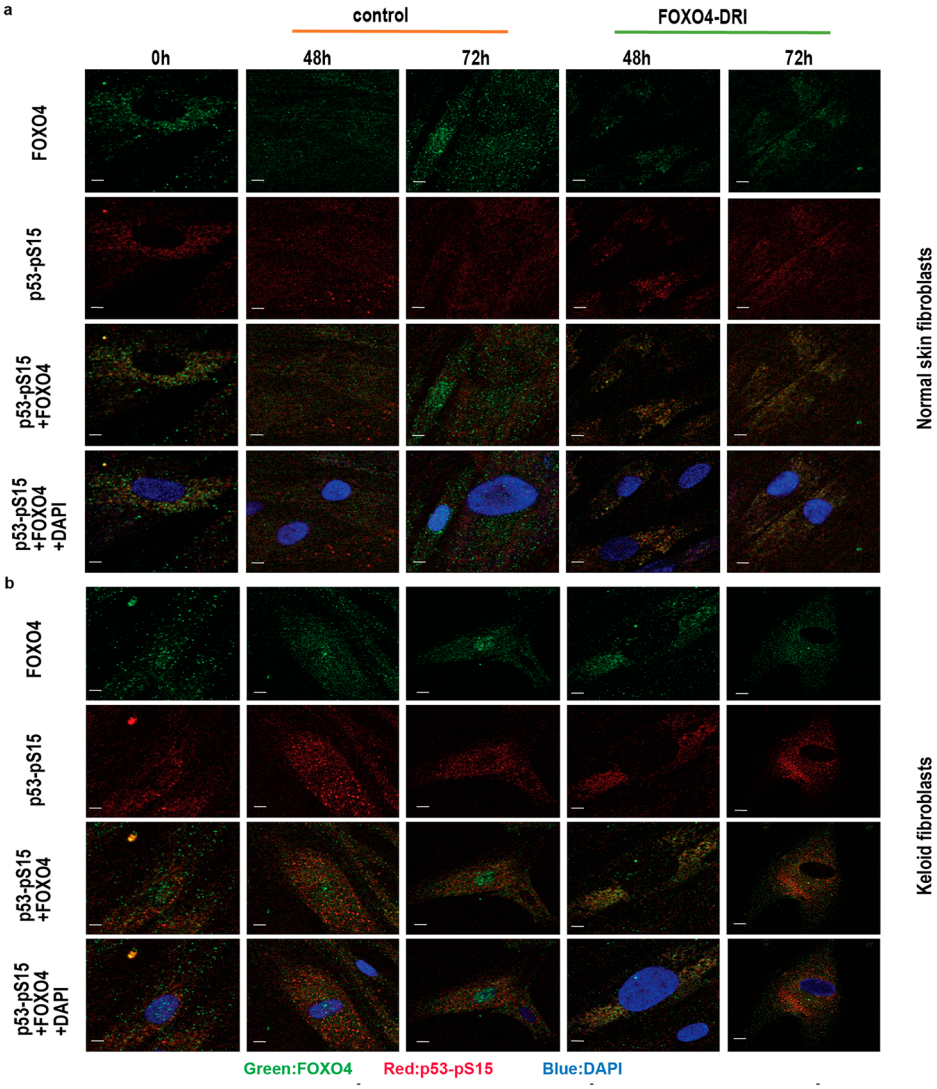

Fig. 7 | Effect of FOXO4-DRI on localization of p53-pS15 and FOXO4 in senescent fibroblast model in vitro. Double immunofluorescence staining of the serum limitation-induced senescent fibroblasts model from normal skin (**a**) and keloid (**b**) with or without FOXO4-DRI (25 μM) in medium for 3 days. p53-pS15 (Red) and FOXO4 (Green). The nucleus was counterstained with DAPI (Blue) (scale bar = 10 μm).

culture medium was added to the wells before a 2 h incubation at 37 °C. Absorbance was measured at 450 nm at an EnSpire multimode plate reader (PerkinElmer, Singapore). The cells in control well were not treated with FOXO4-DRI, and the blank well containing the medium without cells were used to normalized. IC50 was calculated according to cell viability using the nonlinear regression analyses in GraphPad Prism 10.0 software.

Western blot analysis

RIPA Lysis Buffer (TransGen, Beijing, China) was used to extract total protein from tissues/fibroblasts and a Nuclear and Cytoplasmic Protein Extraction Kit (TransGen) was used to extract the protein from nucleus and cytoplasm of fibroblasts. Protein (50 μg) was separated using sodium dodecyl sulfate-polyacrylamide gel electrophoresis on a Precast PAGE Gel (4–12%, APPLYGEN, Beijing, China) and electroblotted onto nitrocellulose membranes. Specific primary antibodies were shown in Table 2, and horseradish peroxidase-conjugated goat anti-mouse or anti-rabbit IgG secondary antibodies (1:4000; Proteintech, Rosemont, IL, USA) were used for western blotting. Protein bands were visualized using Immobilon Western Chemiluminescent HRP Substrate (Merck Millipore, Billerica, MA, USA) and a ChemiDoc MP Imaging System with Image Lab™ Touch Software Version 1.0 (Bio-Rad Laboratories, Hercules, CA, USA). Mouse monoclonal anti-GAPDH antibody (1:1000; Proteintech), anti-ß-actin (1:7000; Proteintech), and anti-TBP antibody (1:500; Solarbio) were used as standards for quantitative analysis of the total, cytoplasm and nuclear proteins.

Immunofluorescence staining

Fibroblasts were fixed, permeabilised, blocked, and incubated overnight at 4 °C with primary antibodies targeting p53-pS15 and FOXO4 shown in Table 2, and developed using Alexa Fluor 488-conjugated donkey anti-

Table 1 | Patient data

Case	Age (years)/Sex	Site	Immunohisto-chemistry analysis	Western blot analysis of tissues and fibroblasts	Organ culture model of keloid tissues	CSP 100 plus phosphoprotein microarray
K 1	35/F	Chest	√	√		
K 2	25/F	Chest	√	√		
K 3	27/F	Chest	√	√		
K 4	27/F	Arm	√	√	√	
K 5	38/F	Abdomen	√	√	√	
K 6	33/F	Earlobe	√	√	√	
K 7	36/F	Chest				√
K 8	20/F	Earlobe		√		
K 9	19/F	Earlobe		√		
K10	28/F	Chest		√		
NS1	41/F	Abdomen	√	√		
NS2	35/F	Back	√	√		
NS3	27/F	Chest	√	√		
NS4	36/F	Chest				√
NS5	35/F	Shoulder		√		
NS6	28/F	Chest		√		
NS7	25/F	Chest		√		

√ the tissues or fibroblasts were used in experiments, *K* keloid, *NS* normal skin, *F* female.

Table 2 | List of primary antibodies used in the study

Primary antibodies	Company	Dilution	IHC	WB	IF	Cat.No
Mouse monoclonal p16[1]	BD Biosciences	1:300	√			51-1325gr
Mouse monoclonal p21[2]	BD Biosciences	1:300	√			Cat. No. 15091A
Mouse monoclonal p53[3]	Cell Signalling Technology	1:300	√			48818
Mouse monoclonal Phospho-p53-(ser15)[4]	Proteintech	1:300	√			67826-1-Ig
Rabbit polyclonal FOXO4[5]	Proteintech	1:300	√			21535-1-AP
Mouse monoclonal p16[6]	Abcam	1:2000		√		Ab108349
Mouse monoclonal p53[3]	Cell Signalling Technology	1:2500		√		48818
Rabbit polyclonal p21[7]	Proteintech	1:2000		√		10355-1-AP
Mouse monoclonal Phospho-p53-(ser15)[4]	Proteintech	1:2000		√		67826-1-Ig
Rabbit polyclonal FOXO4[5]	Proteintech	1:2000		√		21535-1-AP
Mouse monoclonal Phospho-p53-(ser15)[4]	Proteintech	1:100			√	67826-1-Ig
Rabbit polyclonal FOXO4[5]	Proteintech	1:300			√	21535-1-AP

IHC immunohistochemistry analysis, *WB* Western blot analysis, *IF* immunofluorescence staining, *Cat. No* catalogue numbers, √ the antibodies were used in experiments, *BD Biosciences* BD Biosciences, Franklin Lakes, NJ, USA, *Cell Signalling Technology* Cell Signalling Technology, Danvers, MA, USA, *Proteintech* Proteintech, Rosemont, IL, USA, *Abcam* Abcam, Cambridge, UK.
The superscript numbers of the primary antibodies correspond to the reference numbers of the antibody datasheets website links listed below:
1. https://www.bdbiosciences.com/content/bdb/paths/generate-tds-document.us.551153.pdf
2. https://www.bdbiosciences.com/zh-cn/products/reagents/microscopy-imaging-reagents/immunohistochemistry-reagents/purified-mouse-anti-human-p21.554228?tab=product_details
3. https://www.cellsignal.cn/products/primary-antibodies/p53-do-7-mouse-mab/48818
4. https://www.ptglab.co.jp/products/Phospho-P53-Ser15-Antibody-67826-1-Ig.htm
5. http://www.ptgcn.com/Products/FOXO4-Antibody-21535-1-AP.htm(WB/IHC/IF/CoIP)
6. https://www.abcam.cn/products/primary-antibodies/cdkn2ap16ink4a-antibody-epr1473-c-terminal-ab108349.html
7. https://www.ptgcn.com/Products/P21-Antibody-10355-1-AP.htm

mouse immunoglobulin G (1:100; Molecular Probes, Eugene, OR, USA) and Cy3-conjugated sheep anti-rabbit antibodies (1:100; Sigma-Aldrich, St. Louis, MO, USA). The slides were mounted with a solution containing DAPI (Molecular Probes) and imaged using a Leica TCS SP8 laser scanning confocal microscope (Leica Microsystems CMS GmbH, Wetzlar, Germany).

Serum limitation-induced organ culture model of keloids and apoptotic induction of FOXO4-DRI in situ

The keloid tissues were cut into 4-mm diameter cylinders using a corneal trephine for organ culture and cultured in a DMEM containing 2% FBS for 10 days to construct the serum limitation-induced senescent organ culture model of keloid tissues. The keloid tissues for organ culture were firstly incubated in a DMEM containing 10% FBS at 37 °C for 24 h, and the medium was replaced by the DMEM containing 2% FBS, the final concentration of 25 μM FOXO4-DRI was added in the medium immediately. The duration of treatment was 3 days. After treatment, tissues were maintained in 2% FBS DMEM until the 10th days, the medium was changed every 3 days. Untreated tissues in 2% FBS DMEM were used as negative controls. At 0, 3, 7, and 10 days, the tissues were fixed, and cryosections were used for in situ apoptotic staining with terminal deoxynucleotidyl

transferase-mediated dUTP nick-end labeling (TUNEL), according to the manufacturer's instructions (Servicebio, Beijing, China).

Statistics and reproducibility

Statistical significance was determined using independent *t*-test for immunohistochemical and western blot analyses, and one-way analysis of variance for cell cycle and apoptosis detection by GraphPad Prism 7.0 software (GraphPad, Inc., La Jolla, CA, USA). Mean differences were considered as statistically significant when $p < 0.05$. Data are presented as the mean ± SD of three or four biological replicates in three or four independent samples.

Reporting summary

Further information on research design is available in the Nature Portfolio Reporting Summary linked to this article.

Data availability

The scRNA-Seq data (HRA000425) were downloaded from China National Center for Bioinformation (CNCB). All data in Figures are included in this article and its Supplementary Information files.

Received: 7 May 2024; Accepted: 14 February 2025;
Published online: 24 February 2025

References

1. Limandjaja, G. C. et al. The keloid disorder: heterogeneity, histopathology, mechanisms and models. *Front. Cell. Dev. Biol.* **8**, 360 (2020).
2. Tan, S., Khumalo, N. & Bayat, A. Understanding keloid pathobiology from a quasi-neoplastic perspective: less of a scar and more of a chronic inflammatory disease with cancer-like tendencies. *Front. Immunol.* **10**, 1810 (2019).
3. Nangole, F. W., Ouyang, K., Anzala, O., Ogengo, J. & Agak, G. W. Multiple cytokines elevated in patients with keloids: is it an indication of auto-inflammatory disease? *J. Inflamm. Res.* **14**, 2465–2470 (2021).
4. Luo, L., Li, J., Wu, Y., Qiao, J. & Fang, H. Adiponectin, but Not TGF-β1, CTGF, IL-6 or TNF-α, may be a potential anti-inflammation and anti-fibrosis factor in keloid. *J. Inflamm. Res.* **14**, 907–916 (2021).
5. Ladin, D. A. et al. p53 and apoptosis alterations in keloids and keloid fibroblasts. *Wound Repair. Regen.* **6**, 28–37 (1998).
6. Zhang, Q. et al. Tumor-like stem cells derived from human keloid are governed by the inflammatory niche driven by IL-17/IL-6 axis. *PLoS ONE* **4**, e7798 (2009).
7. Liang, Y., Zhou, R., Fu, X., Wang, C. & Wang, D. HOXA5 counteracts the function of pathological scar-derived fibroblasts by partially activating p53 signaling. *Cell Death Dis.* **12**, 40 (2021).
8. Lee, W. J. et al. Mortalin deficiency suppresses fibrosis and induces apoptosis in keloid spheroids. *Sci. Rep.* **7**, 12957 (2017).
9. Pawge, G. & Khatik, G. L. p53 regulated senescence mechanism and role of its modulators in age-related disorders. *Biochem. Pharmacol.* **190**, 114651 (2021).
10. Chambers, C. R., Ritchie, S., Pereira, B. A. & Timpson, P. Overcoming the senescence-associated secretory phenotype (SASP): a complex mechanism of resistance in the treatment of cancer. *Mol. Oncol.* **15**, 3242–3255 (2021).
11. Baar, M. P. et al. Targeted apoptosis of senescent cells restores tissue homeostasis in response to chemotoxicity and aging. *Cell* **169**, 132–147.e16 (2017).
12. Ou, H. L. et al. Cellular senescence in cancer: from mechanisms to detection. *Mol. Oncol.* **15**, 2634–2671 (2021).
13. Varmeh, S. et al. Cellular senescence as a possible mechanism for halting progression of keloid lesions. *Genes Cancer* **2**, 1061–1066 (2011).
14. Limandjaja, G. C., Belien, J. M., Scheper, R. J., Niessen, F. B. & Gibbs, S. Hypertrophic and keloid scars fail to progress from the CD34 - /α-smooth muscle actin (α-SMA) + immature scar phenotype and show gradient differences in α-SMA and p16 expression. *Br. J. Dermatol.* **182**, 974–986 (2020).
15. Darmawan, C. C. et al. Dasatinib attenuates fibrosis in keloids by decreasing senescent cell burden. *Acta Derm. Venereol.* **103**, adv4475 (2023).
16. Liu, X, et al. Single-cell RNA-sequencing reveals lineage-specific regulatory changes of fibroblasts and vascular endothelial cells in keloids [Data set]. *J. Invest. Dermatol.* **142**, 124–135 (2022).
17. Deng, C. et al. Single-cell RNA-seq reveals fibroblast heterogeneity and increased mesenchymal fibroblasts in human fibrotic skin diseases. *Nat. Commun.* **12**, 3709 (2021).
18. Takaya, K., Asou, T. & Kishi, K. Downregulation of senescence-associated secretory phenotype by knockdown of secreted frizzled-related protein 4 contributes to the prevention of skin aging. *Aging***14**, 8167–8178 (2022).
19. Mehdizadeh, M., Aguilar, M., Thorin, E., Ferbeyre, G. & Nattel, S. The role of cellular senescence in cardiac disease: basic biology and clinical relevance. *Nat. Rev. Cardiol.* **19**, 250–264 (2022).
20. Aging, Biomarker, Consortium et al. Biomarkers of aging. *Sci. China Life Sci.* **66**, 893–1066 (2023).
21. Wechter, N. et al. Single-cell transcriptomic analysis uncovers diverse and dynamic senescent cell populations. *Aging* **15**, 2824–2851 (2023).
22. Wang, J., Beauchemin, M. & Bertrand, R. Phospho-Bcl-x(L)(Ser62) plays a key role at DNA damage-induced G(2) checkpoint. *Cell Cycle* **11**, 2159–2169 (2012).
23. Kim, B. J., Ryu, S. W. & Song, B. J. JNK- and p38 kinase-mediated phosphorylation of Bax leads to its activation and mitochondrial translocation and to apoptosis of human hepatoma HepG2 cells. *J. Biol. Chem.* **281**, 21256–21265 (2006).
24. Zinkel, S. S. et al. A role for proapoptotic BID in the DNA-damage response. *Cell* **122**, 579–591 (2005).
25. Otero-Albiol, D. & Carnero, A. Cellular senescence or stemness: hypoxia flips the coin. *J. Exp. Clin. Cancer Res.* **40**, 243 (2021).
26. Lu, F., Gao, J., Ogawa, R., Hyakusoku, H. & Ou, C. Biological differences between fibroblasts derived from peripheral and central areas of keloid tissues. *Plast. Reconstr. Surg.* **120**, 625–630 (2007).
27. Teofoli, P. et al. Expression of Bcl-2, p53, c-jun and c-fos protooncogenes in keloids and hypertrophic scars. *J. Dermatol. Sci.* **22**, 31–37 (1999).
28. Loughery, J., Cox, M., Smith, L. M. & Meek, D. W. Critical role for p53-serine 15 phosphorylation in stimulating transactivation at p53-responsive promoters. *Nucleic Acids Res.* **42**, 7666–7680 (2014).
29. Rayess, H., Wang, M. B. & Srivatsan, E. S. Cellular senescence and tumor suppressor gene p16. *Int. J. Cancer* **130**, 1715–1725 (2012).
30. Sturmlechner, I. et al. p21 produces a bioactive secretome that places stressed cells under immunosurveillance. *Science* **374**, eabb3420 (2021).
31. Yan, L. et al. Inhibition of microRNA-21-5p reduces keloid fibroblast autophagy and migration by targeting PTEN after electron beam irradiation. *Lab. Invest.* **100**, 387–399 (2020).
32. Di Micco, R. et al. Cellular senescence in ageing: from mechanisms to therapeutic opportunities. *Nat. Rev. Mol. Cell. Biol.* **22**, 75–95 (2021).

Acknowledgements

This work was supported by grants from the Chinese Academy of Medical Sciences Innovation Fund for Medical Sciences (CIFMS, grant no. 2021-I2M-1-052) by the Chinese Academy of Medical Sciences and Peking Union Medical College; Capital's Funds for Health Improvement and Research (CFH), (grant no. 2022-1-4041) by the Municipal Commission of Science and Technology; Special Research Fund for Plastic Surgery Hospital, Chinese Academy of Medical Sciences and Peking Union Medical College (YS202018) by the Plastic Surgery Hospital, Chinese Academy of Medical Sciences and Peking Union Medical College; and the National Natural Science Foundation of China (Grant No. 81171817) by the National Natural Science Foundation of China.

Author contributions

Y.X.K., L.Y., and R.X. designed and conceived the study. Y.B.L. and B.P. supervised the study. Y.X.K. and Z.S.L. performed the experiments including immunohistochemical and western blotting detection, model construction and acquired the data. Y.X.K., Z.S.L., and X.F. contributed to the bioinformatic analysis and the statistical analysis. Y.X.K., L.Y., and R.X. wrote and revised the manuscript. All authors reviewed the results and agreed to the published version of the manuscript.

Competing interests

The authors declare no competing interests.

Ethical approval

This study was approved by the Ethics Committee of the Plastic Surgery Hospital (Chinese Academy of Medical Sciences and Peking Union Medical College, Beijing, China; approval number: 2021-179), and informed consent was provided by each patient.

Consent for publication

Not applicable.

Additional information

Supplementary information The online version contains supplementary material available at https://doi.org/10.1038/s42003-025-07738-0.

Correspondence and requests for materials should be addressed to Ran Xiao or Li Yan.

Peer review information *Communications Biology* thanks the anonymous reviewers for their contribution to the peer review of this work. Primary Handling Editors: Keith Syson Chan, Christina Karlsson Rosenthal and Mengtan Xing.